Single-Frequency L5 PPP-RTK with GPS, IRNSS, QZSS and Galileo

Li, W.; Nadarajah, N; Teunissen, P. J.G.; Khodabandeh, A.

Publication date
2015

Document Version
Final published version

Published in
28th International Technical Meeting of the Satellite Division of the Institute of Navigation, ION GNSS 2015

Single-frequency L5 PPP-RTK with GPS, IRNSS, QZSS and Galileo

W. Li[1] , N. Nadarajah[1], P. J. G. Teunissen[1,2] and A. Khodabandeh [1]
[1]*GNSS Research Centre, Curtin University of Technology, Perth, Australia*
[2]*Department of Geoscience & Remote Sensing, Delft University of Technology, Delft, The Netherlands*

Abstract

The concept of PPP-RTK is to achieve integer ambiguity resolution (IAR) at a single GNSS user by providing network-derived satellite phase biases (SPBs) in addition to the standard precise point positioning (PPP) corrections. These corrections enable recovering integerness of user ambiguities, thereby recovering the full capability of the precise carrier-phase observations. This contribution analyzes the capability of single-receiver positioning with IAR using new L5/E5a-frequency observations from GPS, the European Galileo, the Japanese quasi-zenith satellite system (QZSS) and the Indian regional navigation satellite system (IRNSS). In the absence of network products for new systems, especially for IRNSS, we use a small array of multi-GNSS stations to provide a batch of network-derived corrections. These array-aided corrections, comprising estimable combinations of the satellite clocks, first-order slant ionospheric delays as well as the satellite phase biases, are applied to the multi-system single-frequency L5/E5a-observations of the user station. Results from real-data experiments demonstrate that even though standalone PPP-RTK using current L5/E5a-enabled satellite sets of each single system is not possible yet, they effectively contribute to the tightly integrated multi-system PPR-RTK.

1 Introduction

The advent of modernized and new global navigation satellite systems (GNSS) has enhanced the availability of satellite based positioning, navigation, and timing (PNT) solutions. Specifically, it increases redundancy and yields operational back-up or independence in case of failure or unavailability of one system. The Indian regional navigation satellite system (IRNSS), being developed for positioning services in and around India, is the latest addition to the global family of satellite based navigation systems. The proposed constellation will consist of four inclined geosynchronous orbit (IGSO) and three geosynchronous orbit (GEO) satellites transmitting navigation signals in both the L5-band and the lower S-band [1] and sharing only L5-frequency with the American GPS, the European Galileo, and the Japanese quasi-zenith satellite system (QZSS) as highlighted in Table 1. At the time of writing (April-May 2015), only two IGSO and a GEO satellites of IRNSS were transmitting navigation signals. Due to shortage of satellites for IRNSS standalone positioning with present constellation, this contribution analyses integer ambiguity resolution (IAR) enabled precise point positioning by integrating L5-observations of IRNSS with L5/E5a-observations of the other systems.

Frequency Band (Central frequency [MHz])	GPS	Galileo	QZSS	IRNSS
L1/E1 (1575.42)	L1	E1	L1	-
L2 (1227.60)	L2	-	L2	-
L5/E5a (1176.45)	**L5**	**E5a**	**L5**	**L5**
E5b (1207.140)	-	E5b	-	-
E5 (1191.795)	-	E5	-	-
E6/LEX (1278.75)	-	E6	LEX	-
S (2492.028)	-	-	-	S

Table 1. GNSS frequency bands; L5/E5a-frequency band is shared by all four systems considered

Since L5/E5a-frequency is under development even for GPS, only a few studies on L5/E5a-signal quality analysis and its positioning performance using real-data have been reported. The stochastic properties of GPS L5 and GIOVE E5a signals using the geometry-free short and zero baseline analysis has been reported in [2] indicating the interoperability of GPS and Galileo. GPS L5-bias characteristics and the analyses of GPS triple

(L1, L2, and L5) frequency precise point positioning have been reported in [3]. As for the L5-signal of IRNSS system, apart from some simulation studies [4–6], the characterization and identification of L5-signals transmitted by IRNSS-1A are reported in [7] using real observation data recorded by a 30-m high-gain antenna. In [8], it is shown that L5/E5a-signals from different systems have comparable noise characteristics and have better code precision compared to that of L1/E1-signals. It is also demonstrated the interoperability among the GPS, Galileo, QZSS, and IRNSS L5/E5a-signals for positioning and navigation.

PPP-RTK, as a synthesis of precise point positioning (PPP) and network-based real-time kinematic (NRTK), has been demonstrated as an innovative and efficient technique enabling single-station precise positioning with IAR. Apart from the satellite orbit and clock corrections, satellite phase bias (SPB) corrections are also provided to user for recovering the integer nature of ambiguities [9–15]. In the absence of network products for new systems, especially for IRNSS, we use a small *array* of multi-GNSS stations to provide a batch of network-derived corrections [16]. The array-aided method provides corrections, comprising estimable combinations of the satellite clocks, first-order slant ionospheric delays as well as the SPBs [17, 18].

This contribution analyses the array-aided single-frequency PPP-RTK using L5/E5a-observations from GPS, Galileo, QZSS, and IRNSS with special attention given to the interoperability of these systems. Since identical receivers were used in this study, inter-system biases (ISBs) [19] among common frequency observables from different systems did not need to be explicitly modelled [20, 21]. Instead of taking pivot satellites for each system, the user can therefore only take one single pivot satellite for all systems. This tightly integrated processing gives a higher level of redundancy. Using real-data collected in Perth, Australia, we present four-system instantaneous (single-epoch) and multi-epoch, L5/E5a-only PPP-RTK results using array-aided products. Results demonstrate that even though standalone PPP-RTK using current L5/E5a-enabled satellite sets of each system is not possible yet, they effectively contribute to the tightly integrated multi-system PPR-RTK. Furthermore, it is shown that the user's capability of instantaneous ambiguity resolution and positioning is improved with the number of antennas in the array.

(a) Array (b) User I

(c) User II

Figure 1. Array of four antennas (a) and two user antennas ((b) and (c)) in the experiment setup at Curtin University and Attadale, respectively

2 Measurement Campaign

The analyses in this contribution are based on data sets from two measurement campaigns, with an array of four antennas and a user station in each campaign. The array of four antennas (CUT3, CUAA, CUBB, CUCC) for both campaigns was deployed at Curtin University, while user stations were located at Curtin University and Attadale, Western Australia (Figure 1), about 350 m and 8.7 km away from the array, respectively. Array data is used to provide satellite clocks, SPBs, together with ionosphere delay corrections for the user, while user data is used to analyse single-frequency instantaneous IAR and position performance after applying these products. As precise orbits are not yet available for IRNSS, the broadcast ephemeris is used, while for other systems, the precise orbits from the IGS-MGEX campaign are used.

As summarized in Table 2, the first experiment was conducted at Curtin University on April 18, 2015, with the array and a user station (SPA7). Both the reference

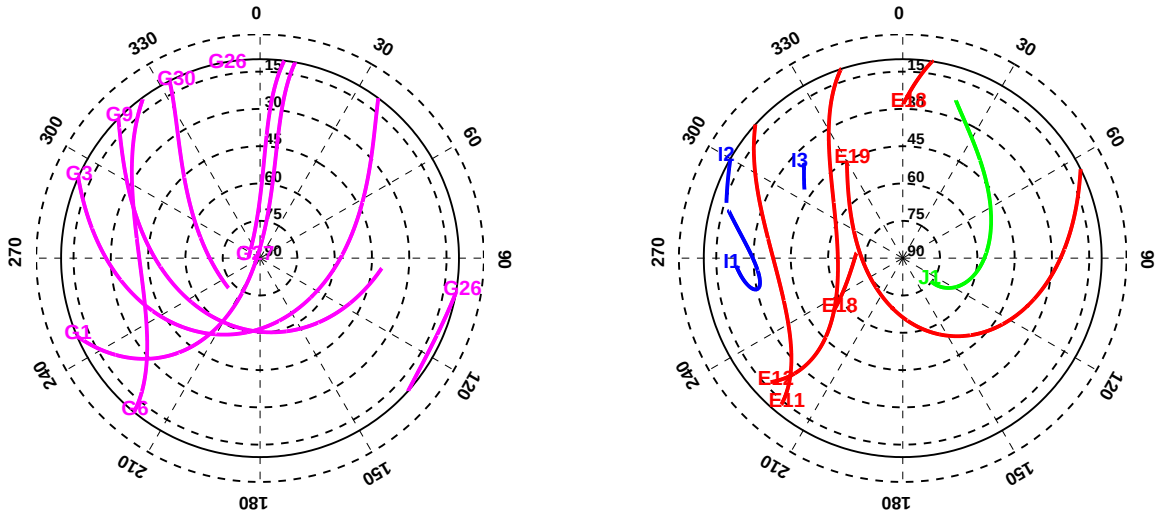

(a) GPS satellites

(b) non-GPS satellites

Figure 2. Experiment I: skyplot of GPS BLOCK II-F (magenta), Galileo (red), QZSS (green) and IRNSS (blue) satellites with L5/E5a-signal in Perth, Australia during the period considered (Table 2), with 10° elevation cutoff

and user stations are equipped with JAVAD TRE_G3TH_8 receivers and connected to TRM 59800.00 antennas. GNSS data was collected for about 9 hours at a rate of 1 Hz (32491 epochs). As shown in the skyplots (Figure 2), L5/E5a-enabled satellites consist of seven GPS Block IIF satellites (G1, G3, G6, G9, G26, G27 and G30), three Galileo in-orbit validation (IOV) satellites (E11, E12, and E19) and a Galileo full operational capability (FOC) satellites (E18), a QZSS satellite (J1) and three IRNSS satellites (I1, I2 and I3). Most of these satellites were in the western side, including three IRNSS satellites, except J1, G3, G9, G26, and E19, which were on the eastern side, therefore improving the receiver-satellite geometry. Figure 3 shows the number of satellites for each GNSS system with L5/E5a-signal and PDOP values with 10° elevation cutoff. Note that the PDOP values correspond to a tightly integrated observation model estimating only one receiver clock error for all combined systems.

The second experiment was conducted on May 8, 2015 collecting GNSS data from the array and a user station at Attadale, Western Australia for about 4.5 hours at a rate of 1 Hz (15668 epochs). As shown in the skyplots (Figure 4), L5/E5a-enabled satellites consist of six GPS Block IIF satellites (G1, G3, G6, G9, G26 and G30), three Galileo IOV satellites (E11, E12, and E19) and a Galileo FOC satellites (E14), a QZSS satellite (J1) and two IRNSS satellites (I1 and I3). The average number of visible satellites with L5/E5a availability is 9, while PDOP value of L5/E5a-enabled satellite set varies from 2 to 4 (Figure 5).

	Array	Exp. I	Exp. II
Location	Curtin Uni.	Curtin Uni.	Attadale
Receiver Type	JAVAD TRE_G3TH_8	JAVAD TRE_G3TH_8	JAVAD TRE_G3TH_8
Antenna Type	TRM 59800.00 SCIS	TRM 59800.00 SCIS	JAV_GRANT-G3T
No. of Antennas	4	1	1
Systems	G, E, J, I	G, E, J, I	G, E, J, I
Sampling Interval	1 sec	1 sec	1 sec
Period of Exp. I	April 18, 2015 (05:55:30-14:57:00 UTC)	April 18, 2015 (05:55:30-14:57:00 UTC)	
Period of Exp. II	May 8, 2015 (06:50:10-11:11:17 UTC)		May 8, 2015 (06:50:10-11:11:17 UTC)

Table 2. Information of array and user data sets in the experiment I & II. G - GPS, E - Galileo, J - QZSS, I - IRNSS

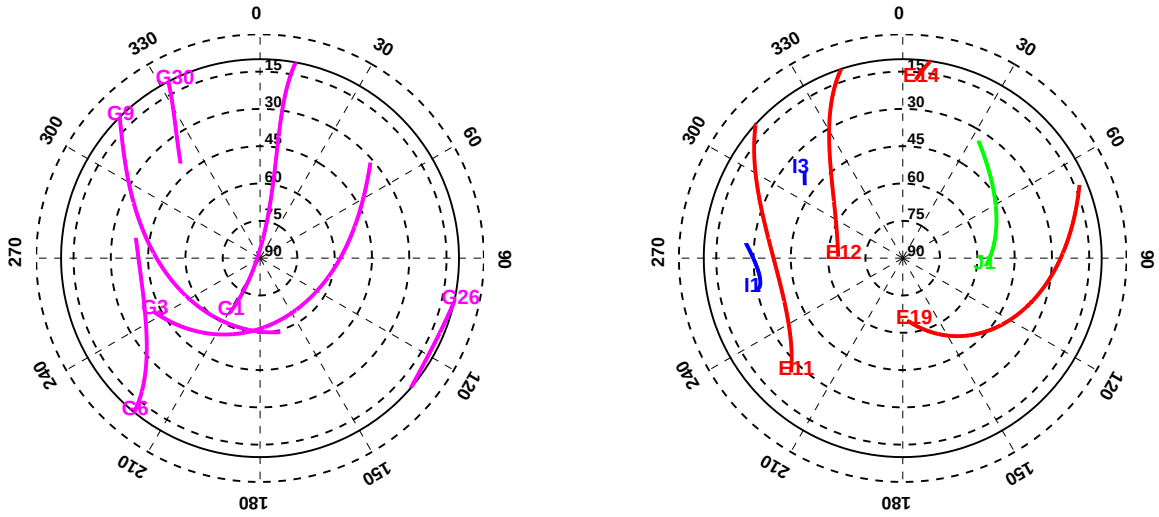

(a) GPS satellites

(b) non-GPS satellites

Figure 4. Experiment II: skyplot of GPS BLOCK II-F (magenta), Galileo (red), QZSS (green) and IRNSS (blue) satellites with L5/E5a-signal in Perth, Australia, with 10° elevation cutoff

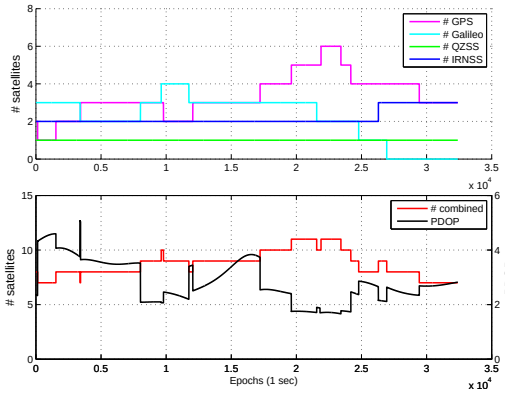

Figure 3. Experiment I: satellite visibility for each GNSS system with L5/E5a-signal (Top), satellite visibility and PDOP for combined systems (Bottom), with 10° elevation cutoff

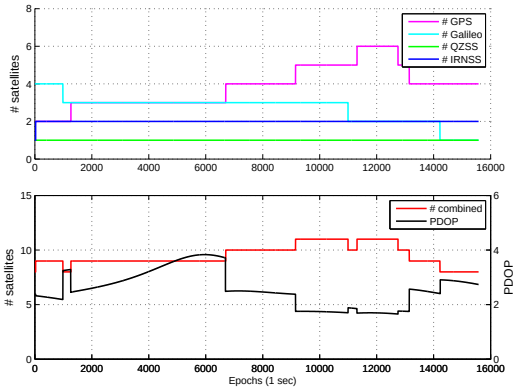

Figure 5. Experiment II: satellite visibility for each GNSS system with L5/E5a-signal (Top), satellite visibility and PDOP for combined systems (Bottom), with 10° elevation cutoff

3 Real-Data Analysis

In this section the performance analysis of array-aided single-frequency PPP-RTK method is presented. First, estimable combinations (corrections) of satellite clocks, SPBs and ionospheric delays of each GNSS system are generated using the data from single-antenna or the array of up to four antennas based on S-system theory [17, 18, 22]. Then, these array-aided corrections are applied to user observations resulting in user observation equations having only user position, receiver clock, receiver phase biases and integer ambiguities as unknowns, hence, enabling precise positioning of the user with IAR [13, 14, 23].

For user positioning performance analyses, first, four-system instantaneous (single-epoch) L5/E5a-only PPP-RTK is considered evaluating instantaneous IAR success rate and instantaneous positioning accuracy. The instantaneous IAR success rate is computed by comparing ambiguities of epoch-by-epoch processing

with the reference ambiguities, which are determined using multi-epoch processing with a Kalman filter assuming ambiguities are constant. Positioning accuracy is given by the root mean squared error (RMSE) with respect to the ground truth, which is determined by ambiguity fixed static relative positioning using GPS dual-frequency data.

Finally, the performance of multi-epoch L5/E5a-only PPP-RTK processing using a Kalman filter is evaluated demonstrating the performance of the filter convergence and positioning accuracy. For filtering, ambiguities and receiver phase bias are assumed time constant, while other parameters such as user position and receiver clock error, are assumed unlinked in time. The full set of float ambiguities of both epoch-by-epoch processing and multi-epoch processing are resolved using the LAMBDA method [24].

3.1 Experiment I

3.1.1 Single-epoch PPP-RTK

In this section, we evaluate the performance of four-system L5/E5a PPP-RTK in an epoch-by-epoch processing of user data from Experiment I with atmosphere-corrected model. Table 3 summarizes empirical instantaneous ambiguity resolution success rates demonstrating improved ambiguity resolution success rate with number of antennas used for array-aided corrections. Figure 6 shows position scatter-plots for both ambiguity float and fixed solutions as a function of number of antennas $n = 1,2,3,4$ demonstrating the effects of number of antennas used for the array-aided PPP-RTK corrections. A zoom-in view of correctly fixed solutions and corresponding 95% confidence ellipsoids are also provided demonstrating that the positioning accuracy of ambiguity fixed solution is driven by precise phase observations.

The positioning accuracy (RMSE) of both float and fixed solutions is provided on the top of the scatter plots in Figure 6 demonstrating improved positioning accuracy, especially for float solution, with number of antennas used for array-aided corrections. The float and correctly fixed position RMSE values are at decimeter and millimeter level, respectively. Figure 7 depicts the histograms of north, east and up components before and after ambiguity fixing matching with the theoretical (normal) distribution.

No. of antennas	Exp. I	Exp. II
$n = 1$	94.6	82.2
$n = 2$	95.2	88.9
$n = 3$	96.6	91.2
$n = 4$	97.1	93.6

Table 3. Empirical instantaneous IAR success rate in percent for single-frequency epoch-by-epoch L5/E5a PPP-RTK from Experiment I & II

.

3.1.2 Multi-epoch PPP-RTK

Figure 8 shows the time series of the four-system L5/E5a-based PPP-RTK ambiguity-float positioning error in north and east component as a function of the number of antennas, with a zoom-in subplot in each figure showing the positioning performance of first 5000 epochs. At beginning of filter, the float positions are dominated by code observations. As the number of antennas n increases, the precision (standard deviation) of SPBs corrections have an improvement of $\sqrt{n}$ [17]; this improved precision of SPBs corrections have also an influence on the convergence time of float positions. For instance as shown in Figure 8(b), the convergence time has reduced from single-antenna corrections to array-aided corrections using an array of four antennas ($n = 4$). After the filter is converged, the time series of all four cases ($n = 1,2,3,4$) have the same tend as the position precision after convergence is driven by precise phase observations.

Position time series of ambiguity-fixed solution are depicted in Figure 9 indicating correct ambiguity fixing from the first epoch and demonstrating the benefit of IAR, especially prominent improvement of the fixed east solution compared to float counterpart. Moreover, the accuracy of ambiguity-fixed position estimates slightly improves with the number of antennas as ambiguity-fixed solutions are driven by precise phase observations. RMSE values of the user position estimates before and after ambiguity fixing is presented in Table 4 highlighting the significant improvement of user position after ambiguity-fixing; moreover, the more antennas are used to provide the corrections, the more improvement of float positions would occur.

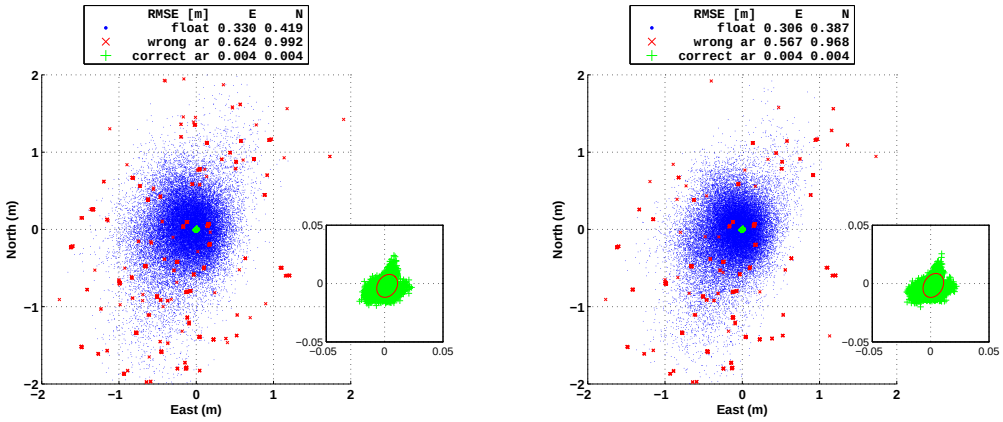

(a) Single-antenna corrections ($n = 1$)

(b) Array-aided corrections ($n = 2$)

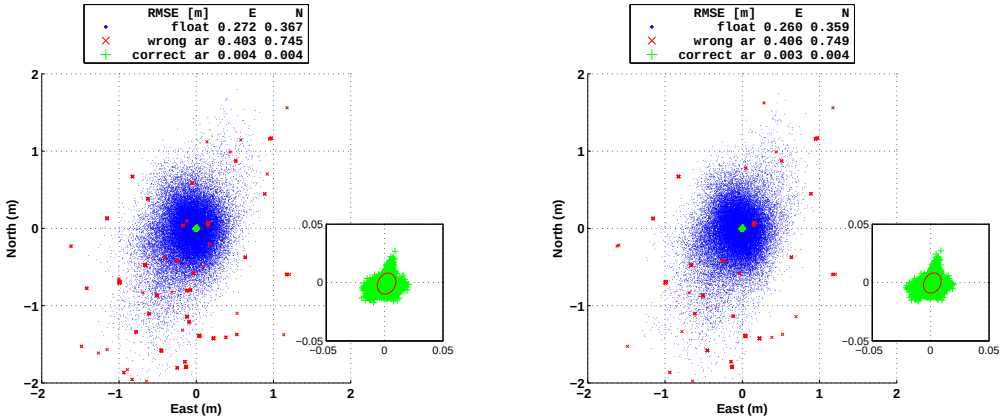

(c) Array-aided corrections ($n = 3$)

(d) Array-aided corrections ($n = 4$)

Figure 6. Experiment I: North-East scatter plot of multi-system L5/E5a PPP-RTK float (blue), wrongly fixed (red) and correctly fixed (green) solutions in a epoch-by-epoch processing, on the basis of array-aided corrections ($n = 1, 2, 3, 4$). The correctly fixed solution and corresponding 95% confidence ellipsoid shown in the zoom-in plot

No of antennas	$n = 1$	$n = 2$	$n = 3$	$n = 4$
North	2.4 (0.5)	2.3 (0.5)	2.2 (0.4)	2.2 (0.4)
East	8.7 (0.4)	6.2 (0.4)	3.7 (0.4)	2.1 (0.3)
Up	4.5 (1.2)	3.8 (1.2)	3.2 (1.1)	2.4 (1.0)

Table 4. Experiment I: RMSE of multi-system L5/E5a float and fixed (in brackets) solution, based on array-aided corrections of different antenna number, in centimeters

3.2 Experiment II

3.2.1 Single-epoch PPP-RTK

Using the four-system L5/E5a observations of Experiment II, the PPP-RTK solution can be computed in epoch-by-epoch processing with instantaneous ambiguity resolution. In the data processing, the ionosphere-weighted model is used to compensate the uncertainty of the slant ionospheric delays between the array and user. Figure 10 shows that the wrongly fixed dots (in red) are less with the number of antennas increasing. After the correct ambiguity fixing, the positioning accuracy of user based on both

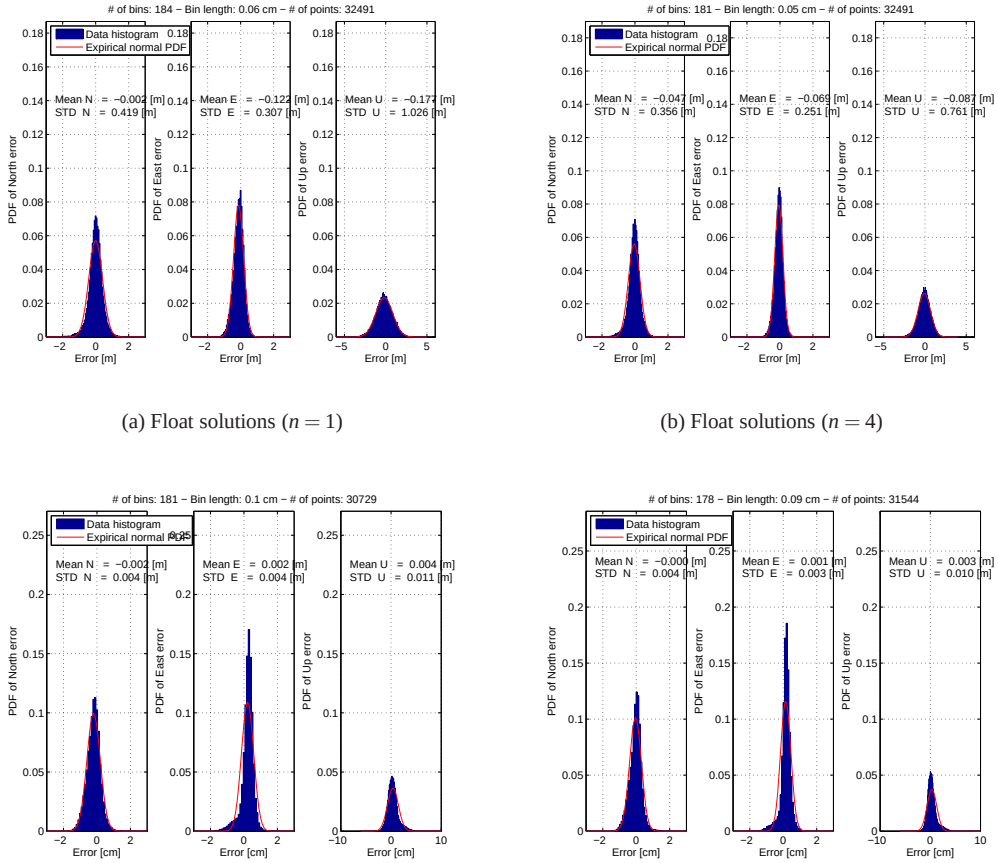

(a) Float solutions ($n = 1$)

(b) Float solutions ($n = 4$)

(c) Fixed solutions ($n = 1$)

(d) Fixed solutions ($n = 4$)

Figure 7. Experiment I: histogram of multi-system L5/E5a PPP-RTK float ((a) and (b)) and correctly fixed ((c) and (d)) positions in a epoch-by-epoch processing, on the basis of single-antenna ($n = 1$) and array-aided corrections ($n = 4$). The corresponding empirical (normal) distribution are shown in red line

single-antenna and array-aided corrections is at mm-cm level, with two order improvement from float solutions of dm-m level.

The instantaneous IAR success rate is summarized in Table 3, which demonstrates a 10% improvement of success rate from single-antenna corrections to array-aided corrections. However, the success rate of Experiment II is lower than Experiment I due to the longer distance from the array and utilization of a weaker (ionosphere-weighted) model.

3.2.2 Multi-epoch PPP-RTK

The filter float and fixed solutions using data sets of Experiment II are illustrated in Figures 11 and 12. Note that the float ambiguities are correctly fixed from the first epoch, resulting in instantaneous centimeter positioning accuracy in the horizontal.

4 Conclusions

In this contribution, the instantaneous (single-epoch) and multi-epoch single-frequency L5/E5a PPP-RTK capabilities of a combined GPS+Galileo+QZSS+IRNSS system were analyzed for the first time. The positioning accuracy of single-epoch PPP-RTK aided by ionospheric delay corrections was shown at mm-cm level after correct ambiguity fixing. While the instantaneous IAR success rate was shown to improve with the number of antennas. The numerical results show 4%-10% improvement of success rate from single-antenna to array-aided corrections. Furthermore, in the multi-epoch PPP-RTK processing, the convergence time of float

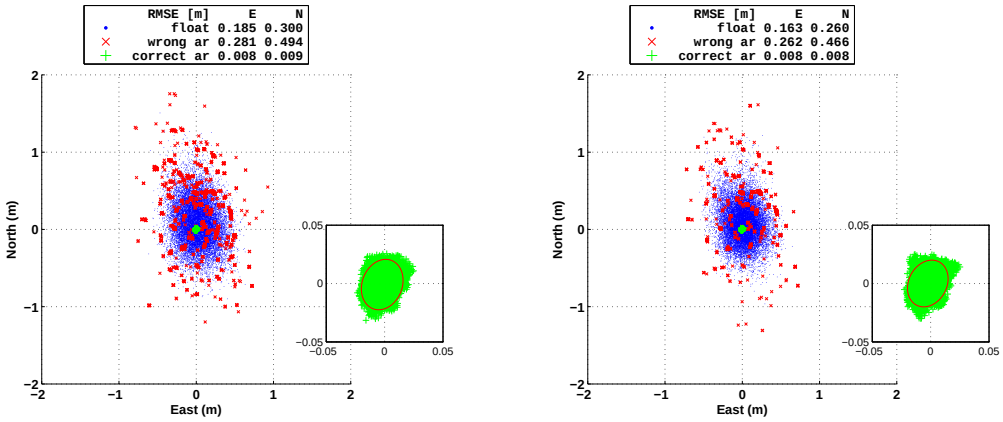

(a) Single-antenna corrections ($n = 1$)

(b) Array-aided corrections ($n = 2$)

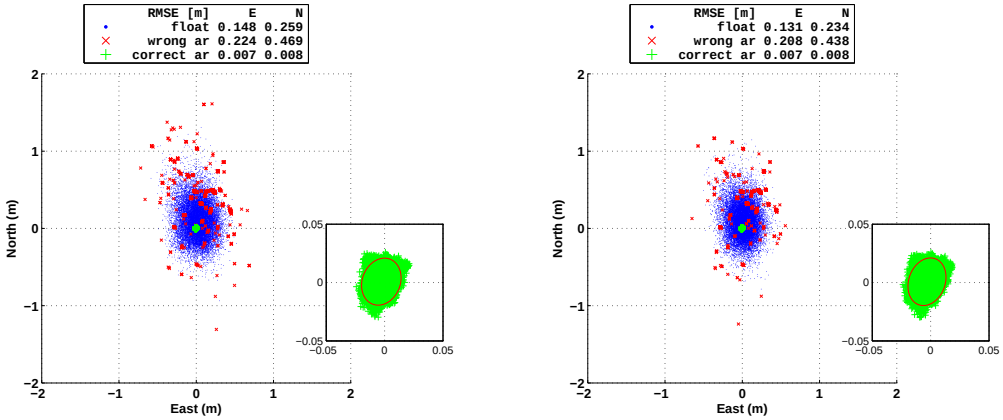

(c) Array-aided corrections ($n = 3$)

(d) Array-aided corrections ($n = 4$)

Figure 10. Experiment II: North-East scatter plot of multi-system L5/E5a PPP-RTK float (blue), wrongly fixed (red) and correctly fixed (green) solutions in the epoch-by-epoch processing, on the basis of array-aided corrections ($n = 1, 2, 3, 4$). The correctly fixed solution and corresponding 95% confidence ellipsoid shown in the zoom-in plot

solutions is also reduced with increasing number of antennas; applying the precise network-derived corrections enables instantaneous ambiguity resolution even with single-frequency L5/E5a observations.

Note that the full L5/E5a-frequency capability is still under development for GPS, Galileo, QZSS and the IRNSS system. Our L5/E5a PPP-RTK results therefore reflect the current positioning performance. After the completion of the full operational L5/E5a satellites, the mean visible number of GNSS satellites increases to 22-28 per epoch with an average PDOP value of 1 (Figure 13). This will therefore improve the L5/E5a PPP-RTK capability significantly.

Acknowledgements

This work has been executed as part of the Positioning Program Project 1.19 Multi-GNSS network PPP-RTK of the Cooperative Research Centre for Spatial Information (CRC-SI). The third author P. J. G. Teunissen is the recipient of an Australian Research Council Federation Fellowship (project number FF0883188). Mr M. Carver, Mr N. Treffers and Dr B. Zhang from Curtin GNSS Research Centre helped us with setting up the second experiment. All this support is gratefully acknowledged.

References

[1] ISRO, "Indian Regional Navigation Satellite System: Signal in space ICD for standard

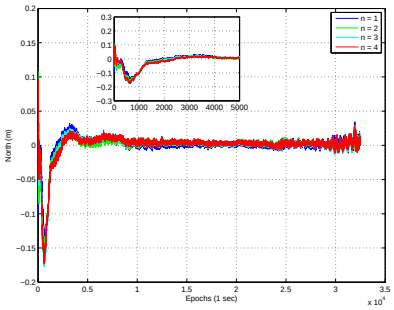

(a) Float solution: north

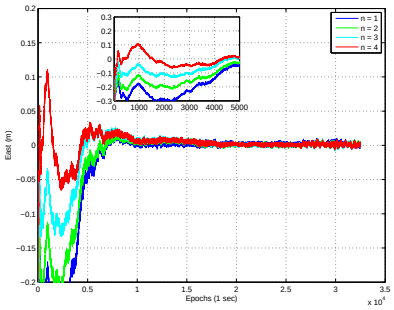

(b) Float solution: east

Figure 8. Experiment I: time series of multi-GNSS L5/E5a PPP-RTK float positions with regard to ground truth, on the basis of single-antenna or array-aided corrections ($n = 1, 2, 3, 4$).

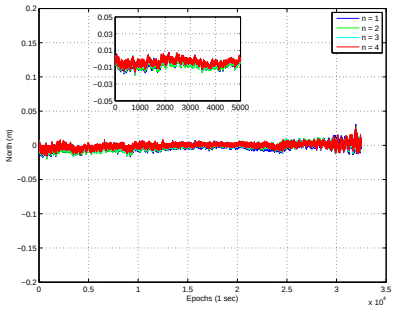

(a) Fixed solution: north

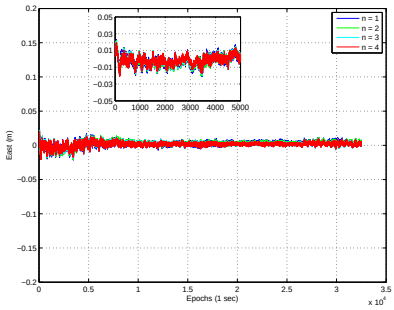

(b) Fixed solution: east

Figure 9. Experiment I: time series of multi-GNSS L5/E5a PPP-RTK fixed positions with regard to ground truth, on the basis of single-antenna or array-aided corrections ($n = 1, 2, 3, 4$).

positioning service," tech. rep., ISRO SATELLITE CENTRE, Bangalore, India, June 2014. Version 1.0.

[2] P. de Bakker, C. Tiberius, H. van der Marel, and R. van Bree, "Short and zero baseline analysis of GPS L1 C/A, L5Q, GIOVE E1B, and E5aQ signals," *GPS Solutions*, vol. 16, pp. 53–64, 2012.

[3] J. Tegedor and O. Øvstedal, "Triple carrier precise point positioning (PPP) using GPS L5," *Survey Review*, vol. 46, no. 337, pp. 288–297, 2014.

[4] V. G. Rao, G. Lachapelle, and S. Vijaykumar, "Analysis of IRNSS over Indian subcontinent," in *Proceedings of the 2011 International Technical Meeting of The Institute of Navigation*, (San Diego), pp. 1150–1162, 2011.

[5] S. B. Sekar, S. Sengupta, and K. Bandyopadhyay, "Spectral compatibility of BOC (5, 2) modulation with existing GNSS signals," in *Position Location and Navigation Symposium (PLANS), 2012 IEEE/ION*, pp. 886–890, IEEE, 2012.

[6] V. Rao, *Proposed LOS fast TTFF signal design for IRNSS*. PhD thesis, University of Calgary, 2013.

[7] S. Thoelert, O. Montenbruck, and M. Meurer, "IRNSS-1A: signal and clock characterization of the Indian regional navigation system," *GPS solutions*, vol. 18, no. 1, pp. 147–152, 2014.

[8] N. Nadarajah, A. Khodabandeh, and P. J. G. Teunissen, "Assessing the IRNSS L5-signal in combination with GPS, Galileo, and QZSS L5/E5a-signals for positioning and navigation," *GPS Solutions*, pp. 1–9, 2015.

[9] G. Wübbena, M. Schmitz, and A. Bagge, "PPP-RTK: precise point positioning using state-space

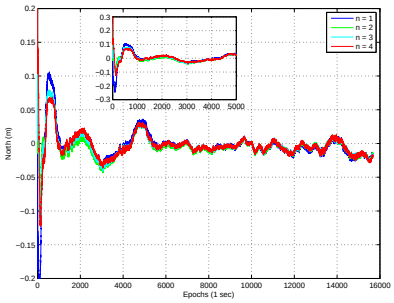

(a) Float solution: north

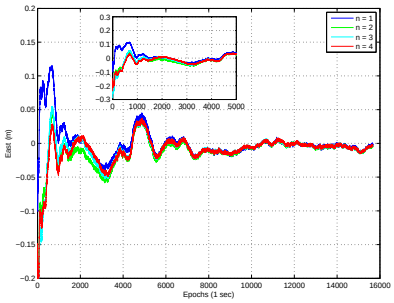

(b) Float solution: east

Figure 11. Experiment II: time series of multi-system L5/E5a PPP-RTK float positions with regard to ground truth, on the basis of single-antenna or array-aided corrections ($n = 1, 2, 3, 4$).

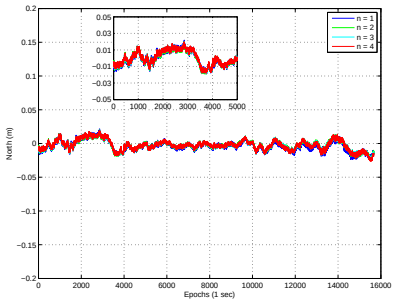

(a) Fixed solution: north

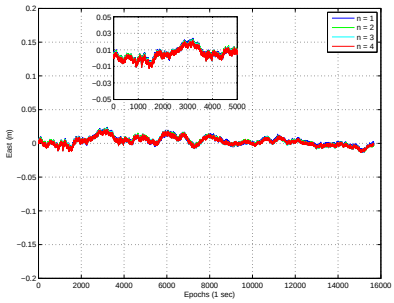

(b) Fixed solution: east

Figure 12. Experiment II: time series of multi-system L5/E5a PPP-RTK fixed positions with regard to ground truth, on the basis of single-antenna or array-aided corrections ($n = 1, 2, 3, 4$).

representation in RTK networks," in *Proceedings of ION GNSS*, vol. 5, pp. 13–16, 2005.

[10] M. Ge, G. Gendt, M. a. Rothacher, C. Shi, and J. Liu, "Resolution of GPS carrier-phase ambiguities in precise point positioning (PPP) with daily observations," *Journal of Geodesy*, vol. 82, no. 7, pp. 389–399, 2008.

[11] D. Laurichesse, F. Mercier, J.-P. BERTHIAS, P. Broca, and L. Cerri, "Integer ambiguity resolution on undifferenced GPS phase measurements and its application to PPP and satellite precise orbit determination," *Navigation*, vol. 56, no. 2, pp. 135–149, 2009.

[12] P. Collins, S. Bisnath, F. Lahaye, and P. Héroux, "Undifferenced GPS ambiguity resolution using the decoupled clock model and ambiguity datum fixing," *Navigation*, vol. 57, no. 2, pp. 123–135, 2010.

[13] P. J. G. Teunissen, D. Odijk, and B. Zhang, "PPP-RTK: Results of CORS Network-Based PPP with Integer Ambiguity Resolution," *Journal of Aeronautics, Astronautics and Aviation. Series A*, vol. 42, no. 4, pp. 223–229, 2010.

[14] B. Zhang, P. J. G. Teunissen, and D. Odijk, "A novel un-differenced PPP-RTK concept," *The Journal of Navigation*, vol. 64, no. Supplement S1, pp. S180–S191, 2011.

[15] J. Geng, C. Shi, M. Ge, A. H. Dodson, Y. Lou, Q. Zhao, and J. Liu, "Improving the estimation of fractional-cycle biases for ambiguity resolution in precise point positioning," *Journal of Geodesy*, vol. 86, no. 8, pp. 579–589, 2012.

[16] P. J. G. Teunissen, "A-PPP: array-aided precise point positioning with global navigation satellite systems," *IEEE Transactions on Signal Processing*, vol. 60, pp. 2870 –2881, June 2012.

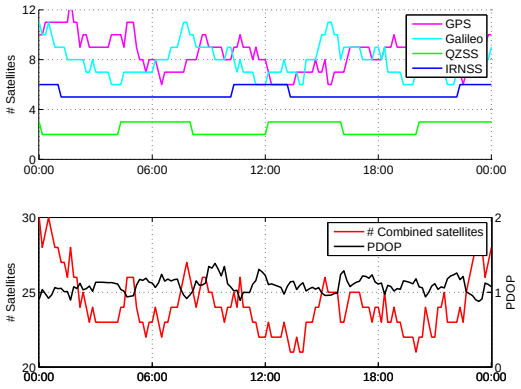

Figure 13. The satellite visibility and geometry of L5/E5a-enabled satellite sets from GPS, Galileo, IRNSS, and QZSS as in Perth, Australia, when all four systems become fully operational by 2020

[17] A. Khodabandeh, "Array-aided single-differenced satellite phase bias determination: methodology and results," in *Proceedings of the 27th International Technical Meeting of the ION Satellite Division (ION GNSS+ 2014)*, (Tampa, Florida), pp. 2523–2532, September 8-12 2014.

[18] A. Khodabandeh and P. J. G. Teunissen, "Array-based satellite phase bias sensing: theory and GPS/BeiDou/QZSS results," *Measurement Science and Technology*, vol. 25, no. 9, p. 095801, 2014.

[19] D. Odijk, P. J. G. Teunissen, and L. Huisman, "First results of mixed GPS+GIOVE single-frequency RTK in Australia," *Journal of Spatial Sciences*, vol. 57, pp. 3–18, June 2012.

[20] D. Odijk and P. J. G. Teunissen, "Characterization of between-receiver GPS-Galileo inter-system biases and their effect on mixed ambiguity resolution," *GPS Solutions*, vol. 17, pp. 521–533, October 2013.

[21] N. Nadarajah, P. J. G. Teunissen, and N. Raziq, "Instantaneous GPS-Galileo attitude determination: single-frequency performance in satellite-deprived environments," *IEEE Transactions on Vehicular Technology*, vol. 62, pp. 2963–2976, September 2013.

[22] P. J. G. Teunissen, "Zero order design: Generalized inverses, adjustment, the datum problem and S-transformations," in *Optimization and Design of Geodetic Networks* (E. W. Grafarend and F. Sansò, eds.), pp. 11–55, Springer Berlin Heidelberg, 1985.

[23] D. Odijk, P. J. G. Teunissen, and B. Zhang, "Single-frequency integer ambiguity resolution enabled precise point positioning," *Journal of Surveying Engineering*, vol. 138, no. 4, p. 193202, 2012.

[24] P. J. G. Teunissen, "The least-squares ambiguity decorrelation adjustment: a method for fast GPS integer ambiguity estimation," *Journal of Geodesy*, vol. 70, pp. 65–82, 1995.